Supplementary Material

Improved Processing Methods for Eddy Covariance Measurements in Calculating Sensible Heat Fluxes at Glacier Surfaces

Cole Lord-May, Valentina Radić

Department of Earth, Ocean and Atmospheric Sciences (EOAS), The University of British Columbia, Vancouver, Canada

Correspondence: Cole Lord-May <clordmay@eoas.ubc.ca>

Meteorological Observations and Surface Energy Balance Closure

Here we elaborate on the meteorological conditions recorded during the observational period, and briefly describe the surface energy balance model used to calculate the modelled melt. All sensors recorded continuously from June 30 to August 27, 2019. Downslope wind was prevalent (82 % of all data was within $\pm 45°$ of downslope, with a median at 265°), with a mean 1 m wind speed of $3.2\,\mathrm{m\,s^{-1}}$ and maximum 30 min wind speeds in excess of $10\,\mathrm{m\,s^{-1}}$ at 3 m (fig. S1 in the supplementary material). Night-time temperatures were an average of 3 °C and day-time temperatures were an average of 7 °C on sunny days. A cumulative 55.1 mm of rain was recorded over the observational period, with the majority occurring over one week in late July. Net shortwave radiation peaked at $600\,\mathrm{Wm^{-2}}$ during clear days and in total there were 47 clear-sky days observed. During clear-sky conditions, EC-derived sensible heat flux was more than an order of magnitude larger than EC-derived latent heat flux (fig. S1). However, when air temperatures are near zero, the latent heat flux can be larger than the sensible heat flux, as was observed in the last week of August. As all sensors were installed after bare ice was exposed, there was a minimal change in the appearance of the glacier surface over the observational period. The exposed ice was fairly dirty with an average albedo of 0.23.

We assess the total energy available for melting, Q_M, through a simple surface energy balance model

for a surface at melting point,

$$Q_M = SR_{\text{down}} - SR_{\text{up}} + LR_{\text{down}} - LR_{\text{up}} + Q_H + Q_L + Q_R + Q_G, \tag{1}$$

consisting of a balance between incoming shortwave (SR_{down}), reflected shortwave (SR_{up}), incoming longwave (LR_{down}), outgoing longwave (LR_{up}), sensible heat flux (Q_H), latent heat flux (Q_L), rain heat flux (Q_R), and ground heat flux (Q_G). For more details, the reviewer is referred to Fitzpatrick and others, 2017.

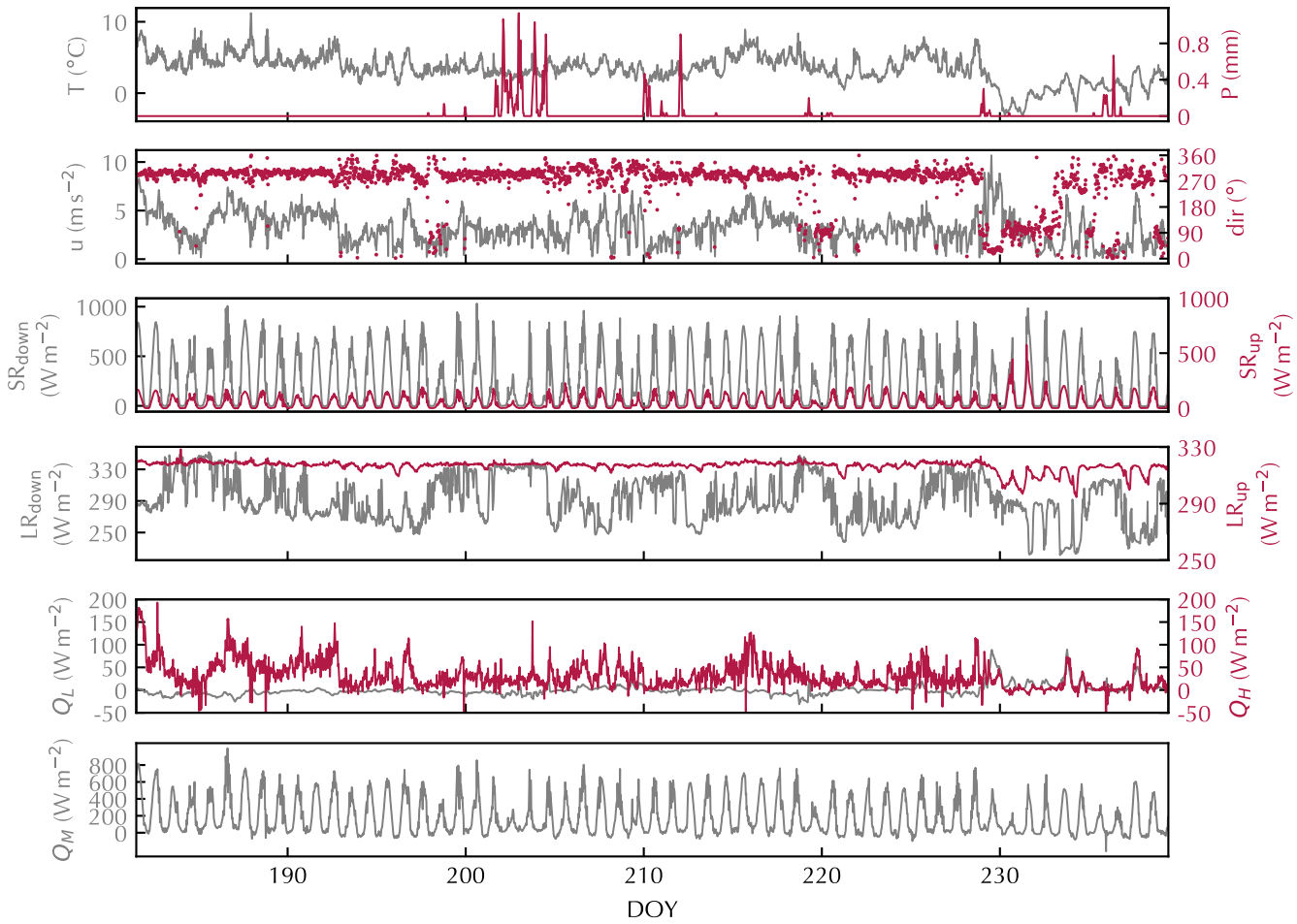

Fig. S1. 30 min averages of meteorological measurements and fluxes at the glacier surface throughout the observational period. T is temperature at 1 m, P is liquid precipitation, U is wind speed at 1 m and *dir* is wind direction, with 270◦ being approximately downslope. SR_{down} and SR_{up} and incoming and reflected shortwave radiation, respectively. LR_{down} and LR_{up} and incoming and outgoing longwave radiation, respectively. Q_H and Q_L are EC-derived sensible and latent heat fluxes at 1 m, calculated here with 30 min averaging windows.

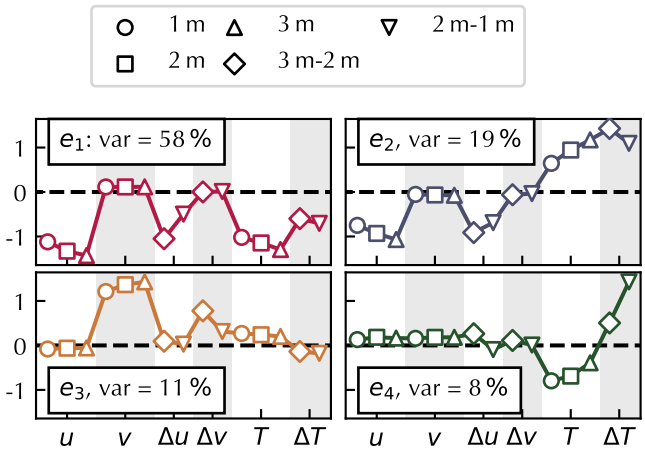

Fig. S2. Eigenvectors e_i of the first four modes in the data consisting of the following variables: u – downslope wind at 1 m, 2 m, 3 m, v – cross-slope wind at 1 m, 2 m, 3 m, Δu – finite difference of downslope wind between 2 m and 1 m, and 3 m and 2 m, Δv: finite difference of downslope wind between 2 m and 1 m, and 3 m and 2 m T – cross-slope wind at 1 m, 2 m, 3 m, and ΔT – finite difference of downslope wind between 2 m and 1 m, and 3 m and 2 m. Circles, squares, and upright triangles denote measurements made at 1 m, 2 m, and 3 m, respectively. Diamonds correspond to a finite difference between 2 m and 1 m, and inverted triangles correspond to a finite difference between 3 m and 2 m. Var indicates how much variance is explained by each mode. Alternating white and grey shading is for visual clarity.

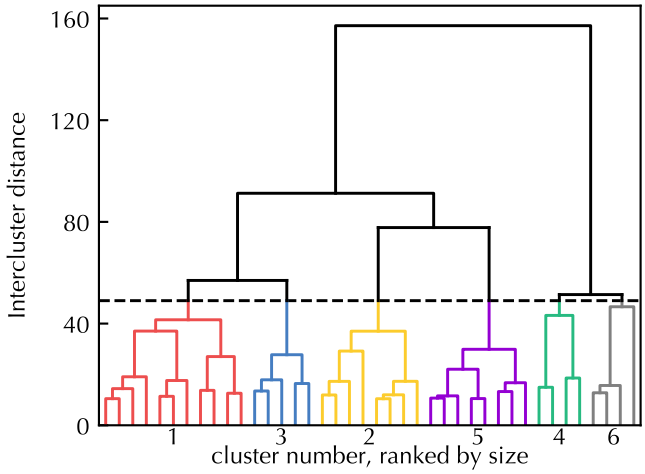

Fig. S3. Dendrogram showing the outcome of hierarchical clustering algorithm and the six selected clusters. In this inverted tree, solid horizontal lines show the merging of two clusters or data points (vertical lines below the horizontal line) into one larger cluster (vertical line above the horizontal line) on the basis of cluster similarity. Intercluster distance is a measure of cluster similarity, with smaller vertical distances, i.e., shorter vertical lines, indicating more similar clusters. The dashed line indicates the intercluster distance selected to generate six clusters. Clusters are colored and numbered according to size with cluster 1 (red) being the largest. Clusters are truncated on the bottom of the plot (not all data points are shown) for visual clarity.

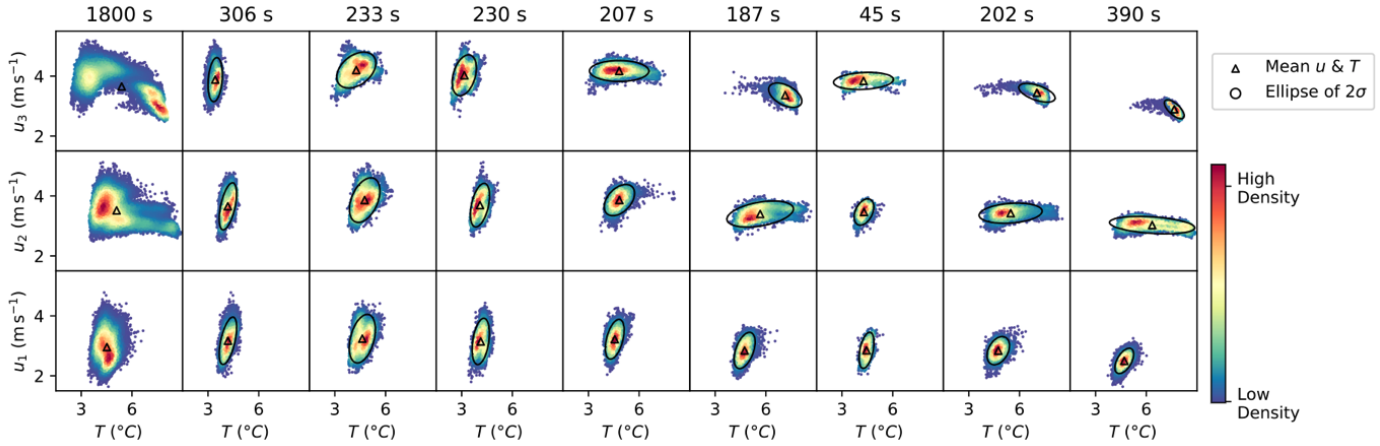

Fig. S4. High frequency scatters of u and T at 1 m (bottom), 2 m (middle), and 3 m (top) during one 30 min record classified as shallow katabatic. The leftmost column shows the scatter over the full 30 min period, and each subsequent column shows the scatter over each CPD-determined averaging interval. Colors indicated a relative point density. The flat ellipses at 2 m in the rightmost two columns indicate a WSM very near 2 m. Flat ellipses, indicating a WSM, are also observed at 3 m other columns of this record.

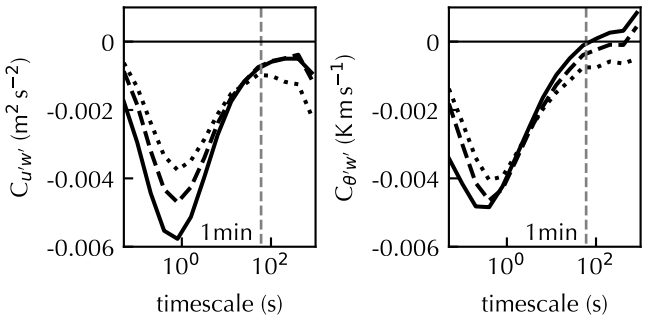

Fig. S5. Contributions to the momentum flux (left) and sensible heat flux (right) as a function of timescale, established with MRD, at 1 m (solid), 2 m (dashed), 3 m (dotted).

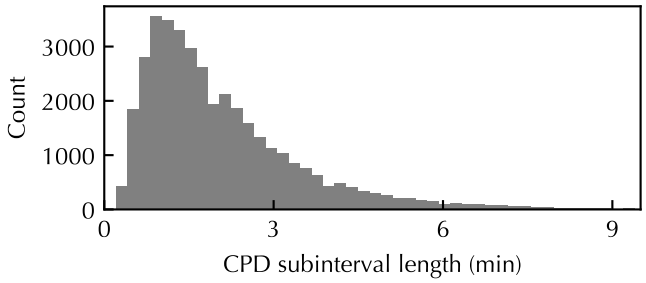

Fig. S6. Distribution of subinterval lengths as calculated with CPD.

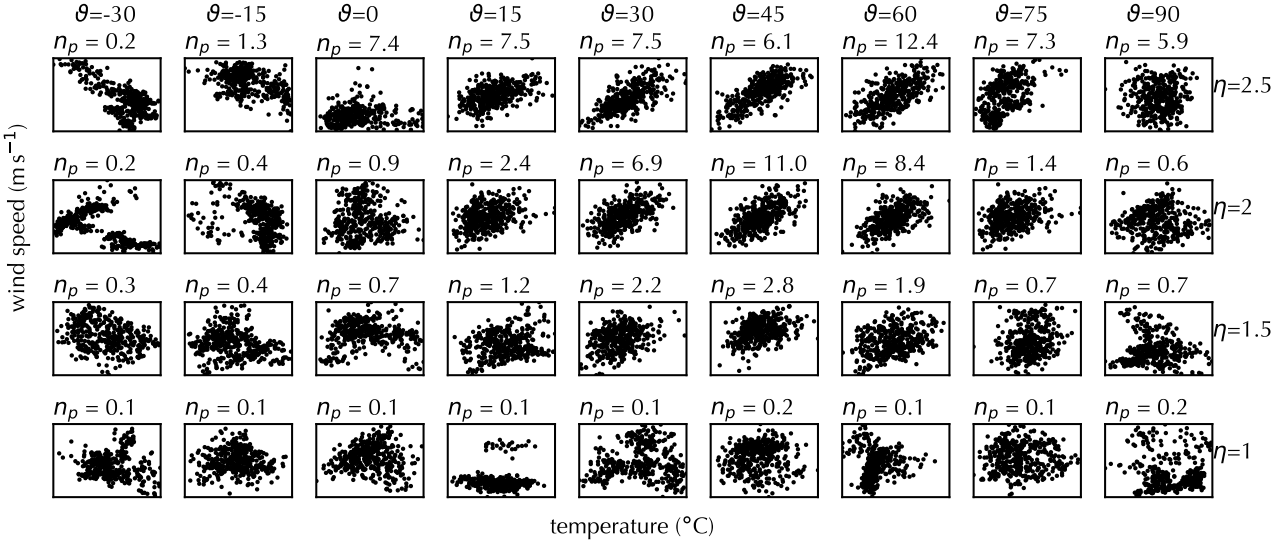

Fig. S7. Representative $T' - u'$ scatter plots over a sweep of ϑ and η from EC measurements at 3 m. Values are omitted in the subplots as the focus is on the shape of the scatter rather than on absolute values. The scales for wind speed and temperature are not consistent among the subplots because they vary substantially. n_p shows the percentage of data that falls into a given $\vartheta - \eta$ bin. To capture ellipsoidal flattening, the unitless widths are equal to the unitless heights of each subplot. For example, a subplot with temperature ranging from 3 °C to 7 °C ($\Delta T = 4$ °C) might show a wind speed range from 6 ms^{-1} to 10 ms^{-1} ($\Delta u = 4$ ms^{-1})

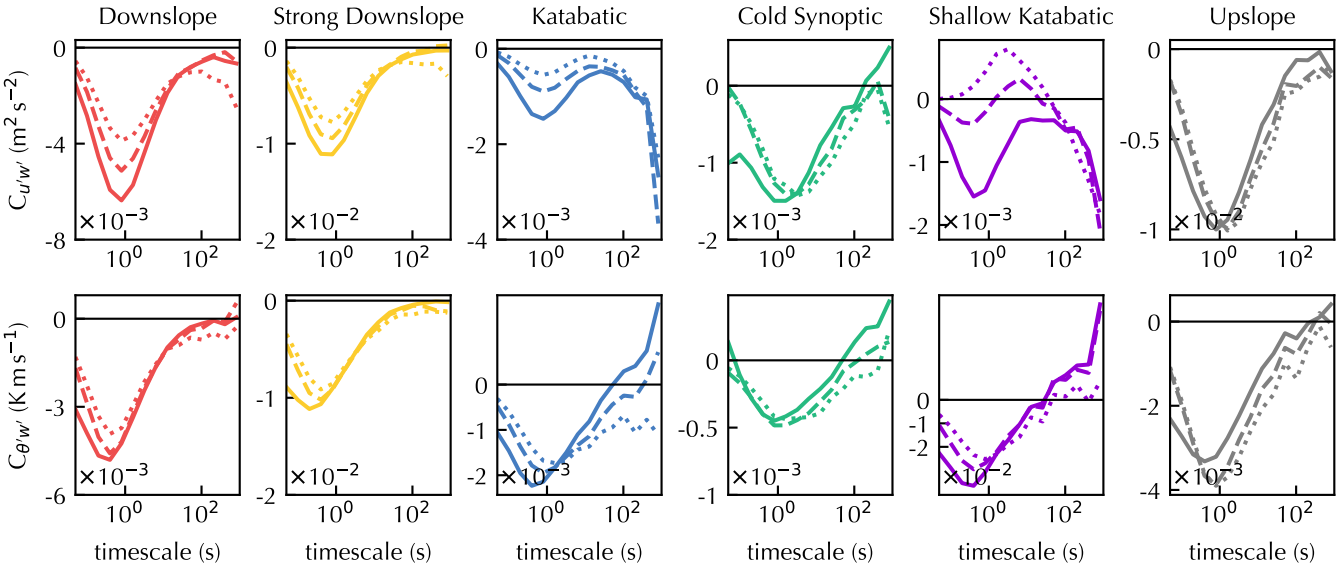

Fig. S8. The same as fig. S5, but separated by flow regime. 1 m (solid), 2 m (dashed), 3 m (dotted). Some regimes, such as 'cold synoptic', show a clear zero-crossing for both momentum and heat flux. Others, such as momentum flux in the 'katabatic' regime, do no show a zero crossing. In this case, we take the location of the local maximum to establish a regime-specific gap scale.